Electronic Supplementary Material (ESI) for Journal of Materials Chemistry A.

Electronic Supplementary Information

Lithium electrodeposited on Lithiophilic LTO/Ti_3C_2 substrate as a Dendrite-free Lithium Metal Anodes

*Ruiyi Gan,[a] Yiling Liu,[a] Na Yang,[a] Cheng Tong,[a] Mingming Deng,[a] Qin Dong,[a] Xianyi Tang,[a] Na Fu,[a] Cunpu Li [*a] and Zidong Wei [*a]*

[a]National-municipal Joint Engineering Laboratory for Chemical Process Intensification and Reaction, School of Chemistry and Chemical Engineering, Chongqing University, Chongqing 400044, China

1. SUPPORTING FIGURES

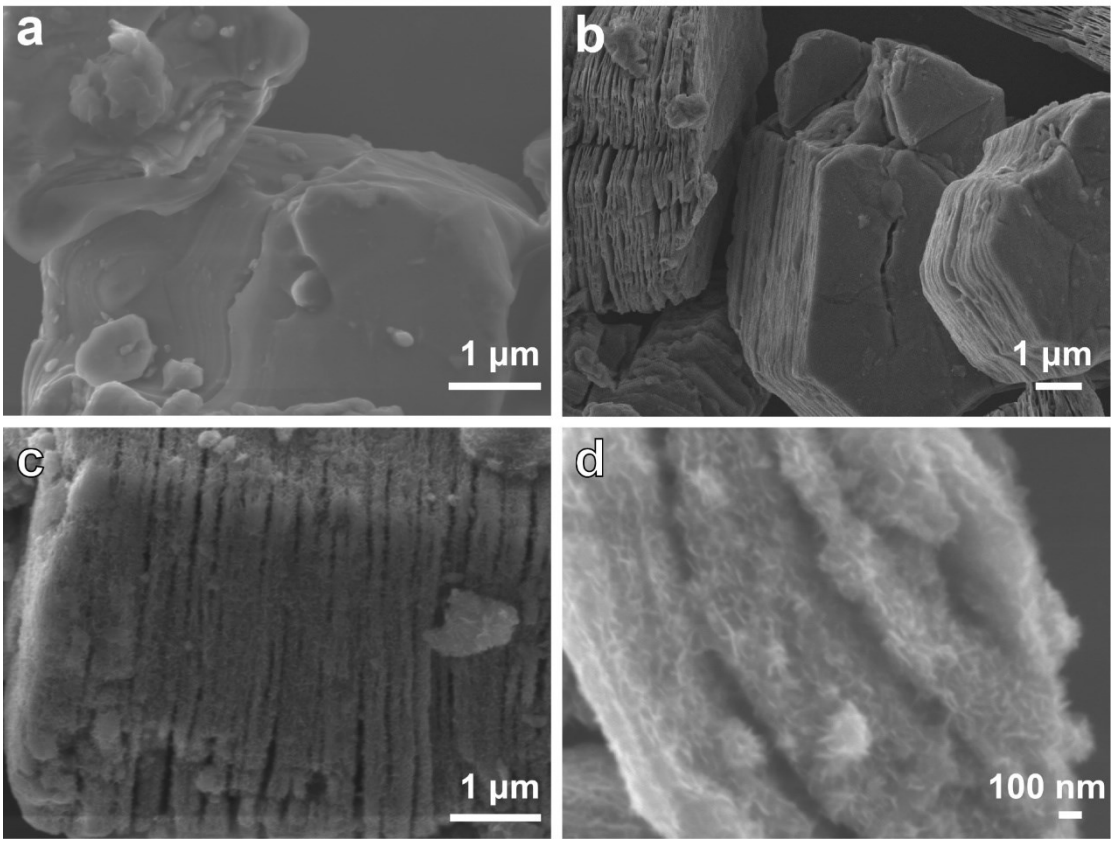

Figure S1. SEM images of (a) Ti_3AlC_2; (b) Ti_3C_2; (c) side view and (d) top view of LTO/Ti_3C_2.

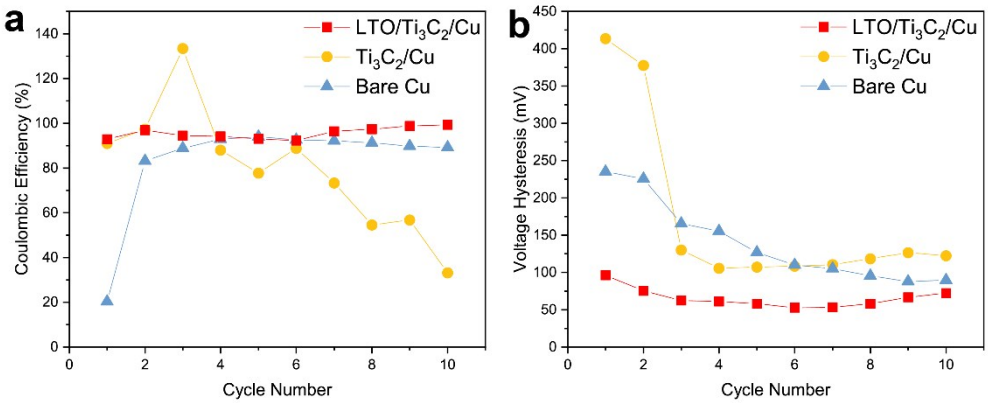

Figure S2. (a) coulombic efficiency evolution and (b) voltage hysteresis evolutions of 10 depositing/stripping cycles on LTO/Ti_3C_2/Cu, Ti_3C_2/Cu, and bare Cu electrodes at a current density of 2 mA·cm^{-2} and a Li depositing capacity of 8 mAh·cm^{-2}.

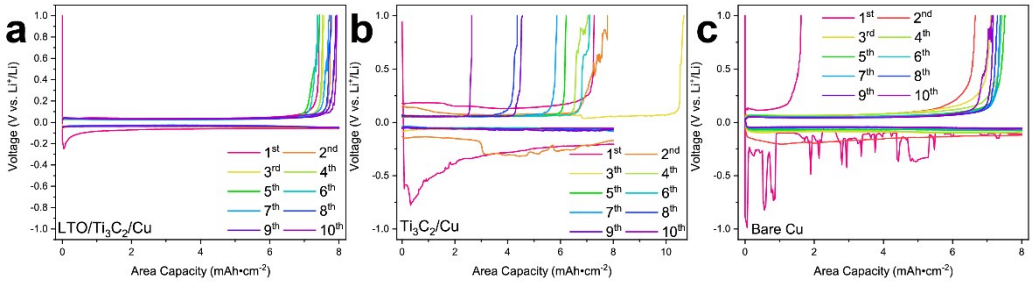

Figure S3. Voltage profiles of Li depositing/stripping on (a)LTO/Ti_3C_2/Cu, (b)Ti_3C_2/Cu, and (c)bare Cu electrodes at a current density of 2 mA·cm^{-2} and a Li depositing/stripping capacity of 8 mAh·cm^{-2} for 10 cycles.

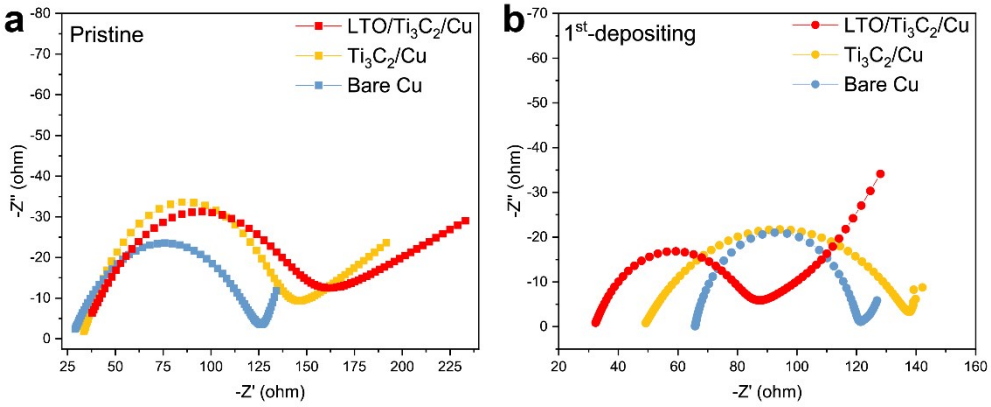

Figure S4. Nyquist plots at frequencies from 10^3 kHz to 100 mHz (a) of pristine batteries and (b) after 1st depositing.

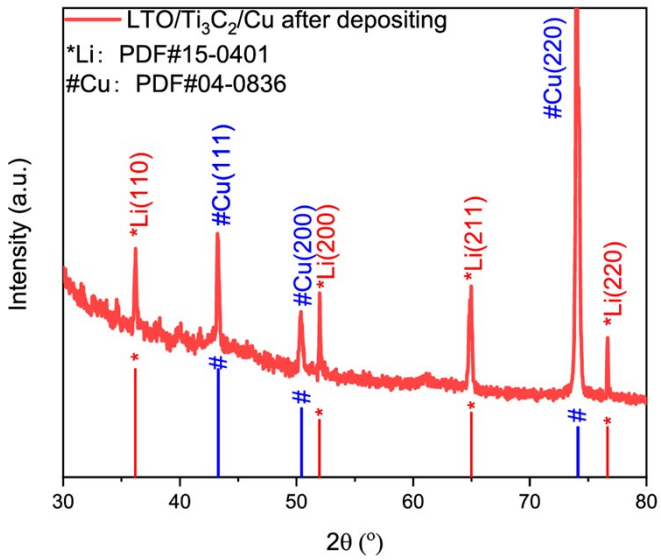

Figure S5. XRD pattern of LTO/Ti_3C_2/Cu electrode after depositing 8 mAh·cm^{-2} of Li.

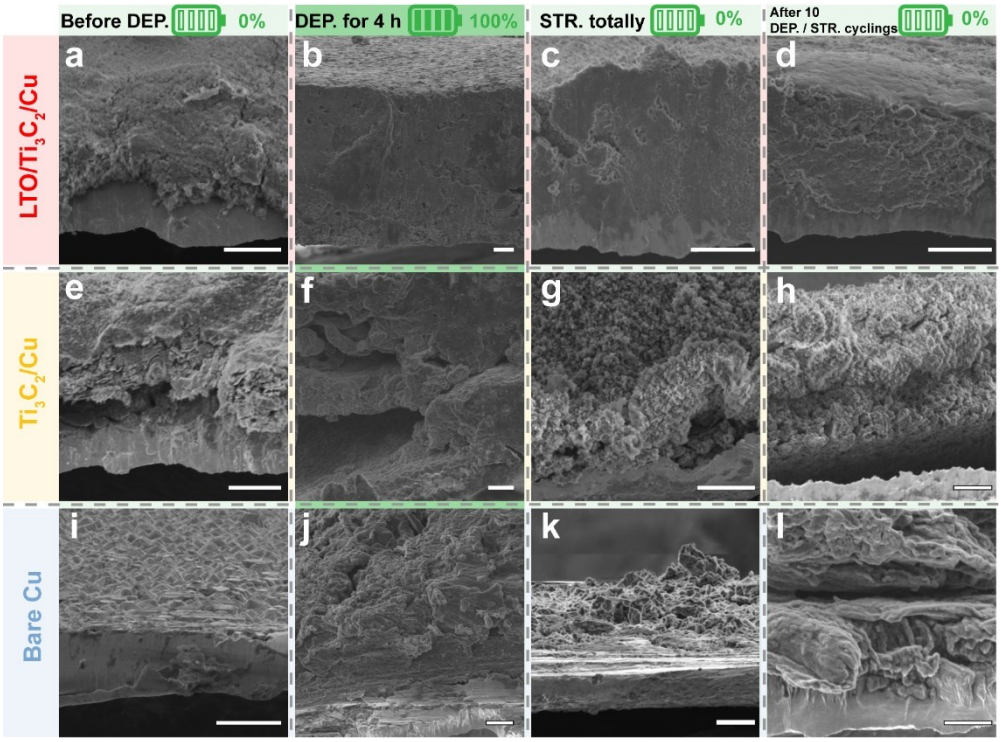

Figure S6. The cross-section SEM images of the LTO/Ti_3C_2/Cu, Ti_3C_2/Cu, and bare Cu electrodes with different Li amounts at a current density of 2 mA·cm^{-2} in the Li deposition/stripping (abbreviated to DEP./STR.) process. The pristine (a) LTO/Ti_3C_2/Cu, (e) Ti_3C_2/Cu, and (i) bare Cu electrodes before cycling. (b) LTO/Ti_3C_2/Cu, (f) Ti_3C_2/Cu, and (j) bare Cu electrodes after the deposition of 8 mAh·cm^{-2} of Li. (c) LTO/Ti_3C_2/Cu, (g) Ti_3C_2/Cu, and (k) bare Cu electrodes after 8 mAh·cm^{-2} of stripping (charged back to 1.0 V) of Li. (d) LTO/Ti_3C_2/Cu, (h) Ti_3C_2/Cu, and (l) bare Cu electrodes after 10 cycles of Li deposition/stripping. The battery icons refer to the amounts of Li in each stage. The scare bars are 10 μm for this figure.

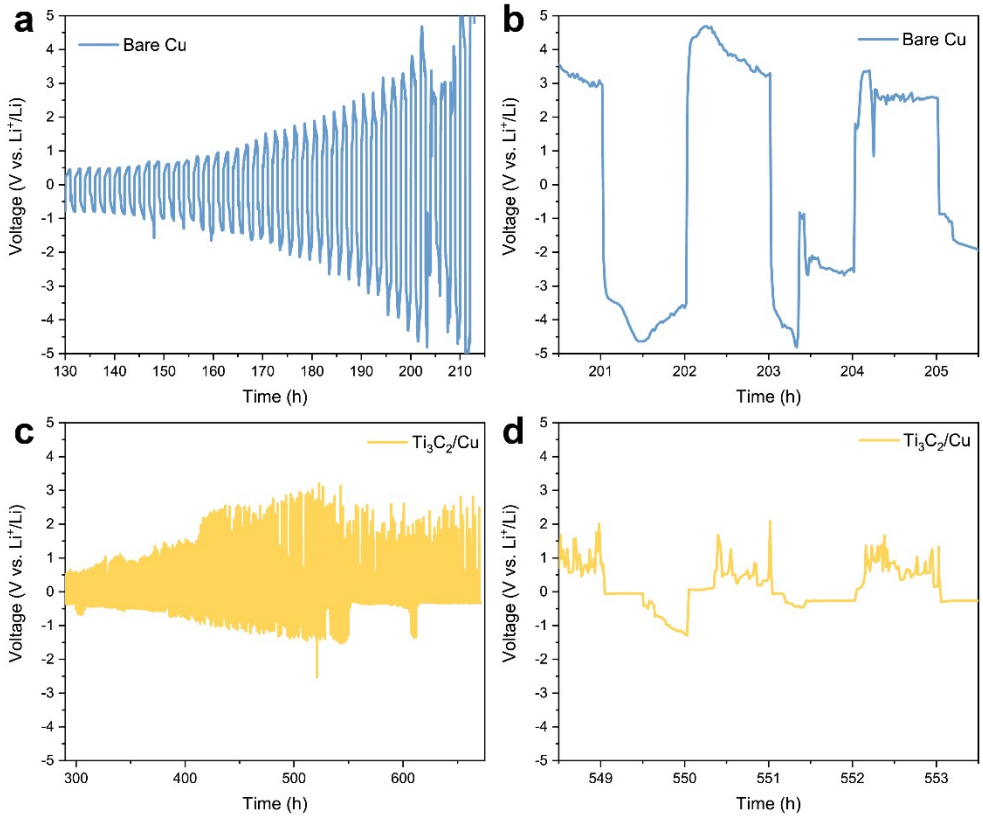

Figure S7. Long-term symmetric galvanostatic charge-discharge voltage profiles of Li|Li/bare Cu for (a) 130 h to shut down and (b) 200.5-205.5 h; and Li|Li/Ti_3C_2/Cu batteries for (c) 290 h to shut down and (d) 548.5-553.5 h at a current density of 1 mA·cm^{-2} with a depositing/stripping capacity of 1 mAh·cm^{-2}.

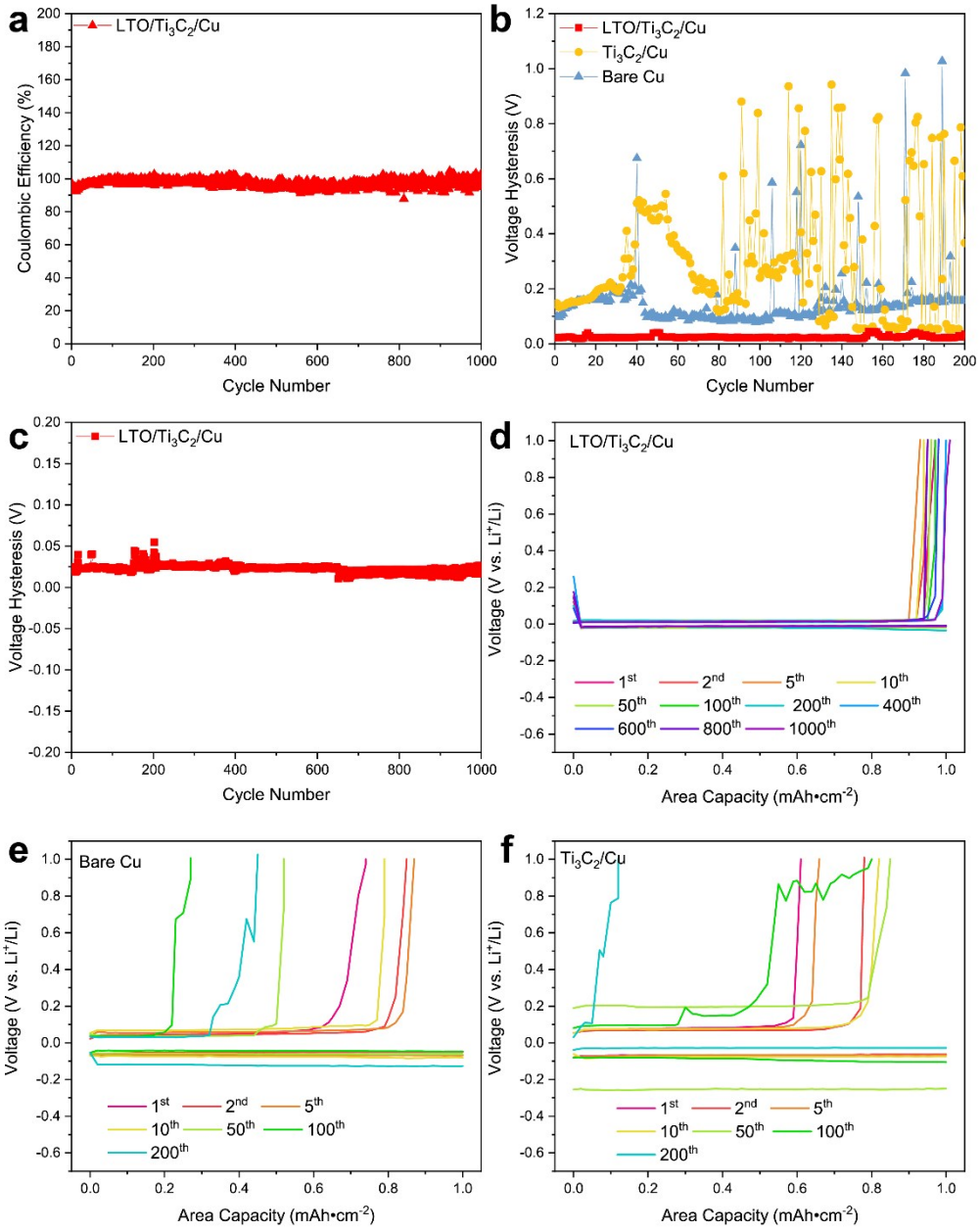

Figure S8. long-term symmetric galvanostatic discharge for 1 h and charge to 1 V at a current density of 1 mA·cm^{-2}: (a) coulombic efficiency of Li|Li/LTO/Ti_3C_2/Cu batteries for 1000 cycles; (b) voltage hysteresis evolutions of Li|Li/LTO/Ti_3C_2/Cu, Li|Li/bare Cu, and Li|Li/Ti_3C_2/Cu batteries for 200 cycles; and (c) voltage hysteresis evolutions of Li|Li/LTO/Ti_3C_2/Cu batteries for 1000 cycles; voltage profiles of (d) Li|Li/LTO/Ti_3C_2/Cu, (e) Li|Li/bare Cu, and (f) Li|Li/Ti_3C_2/Cu batteries.

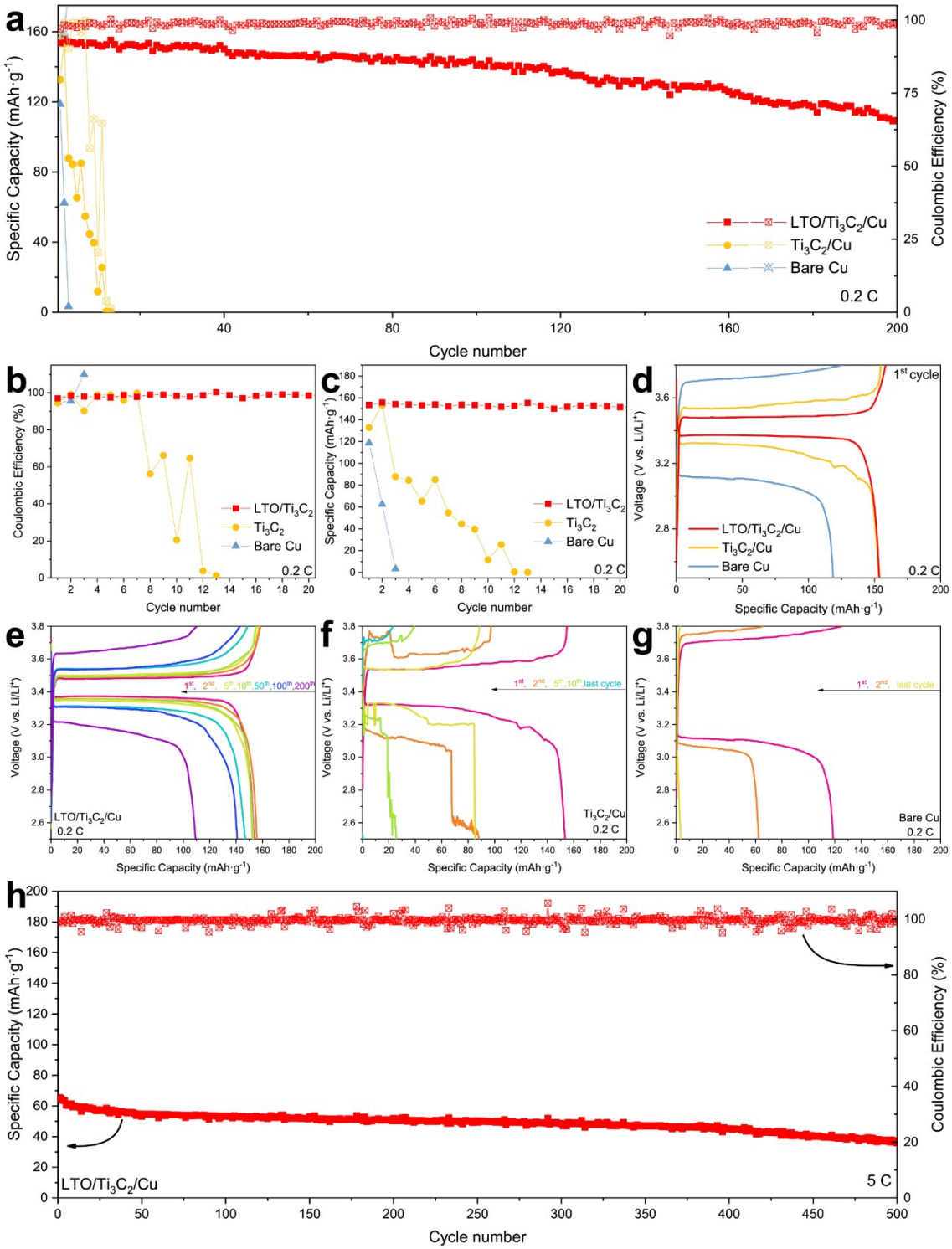

Figure S9. Electrochemical performances of the Li/Bare Cu|LFP, Li/Ti_3C_2/Cu|LFP and Li/LTO/Ti_3C_2/Cu|LFP batteries at 0.2C: (a) the discharge specific capacity and Coulombic efficiency; (b) discharge specific capacity and (c) Coulombic efficiency for the first 15 cycles; galvanostatic charge-discharge curves of (d) three different batteries at 1st cycle, (e) Li/LTO/Ti_3C_2/Cu|LFP, (f) Li/Ti_3C_2/Cu|LFP, and (g) Li/Bare Cu|LFP batteries. (h) Long term cycling performance of Li/LTO/Ti_3C_2/Cu|LFP batteries at 5 C.

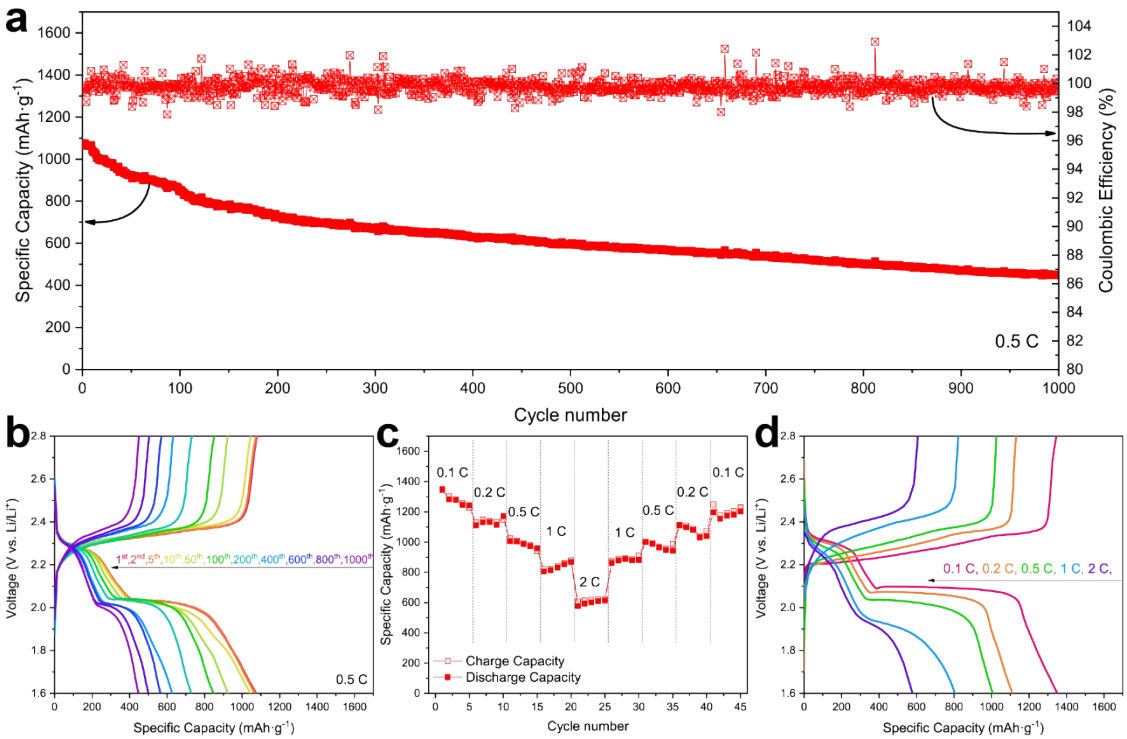

Figure S10. Electrochemical performance of the Li/LTO/Ti_3C_2/Cu|S batteries: (a) long-term cycling performance for 1000 cycles at 0.5 C; (b) galvanostatic charge-discharge curves at 0.5 C for 1000 cycles; (c) cycling performance and (d) galvanostatic charge-discharge curves at different rates from 0.1 C to 2 C.

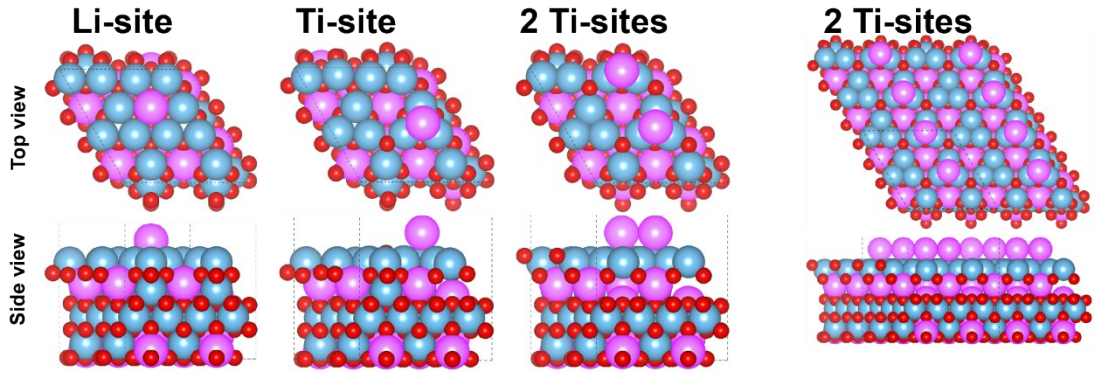

Figure S11. Optimized geometries of Li on $Li_4Ti_5O_{12}$ Ti top (111) slab model surfaces and corresponding adsorption energies, respectively. The atoms are colored as follow: Li is green, Ti is blue, C is grey, and O is red.

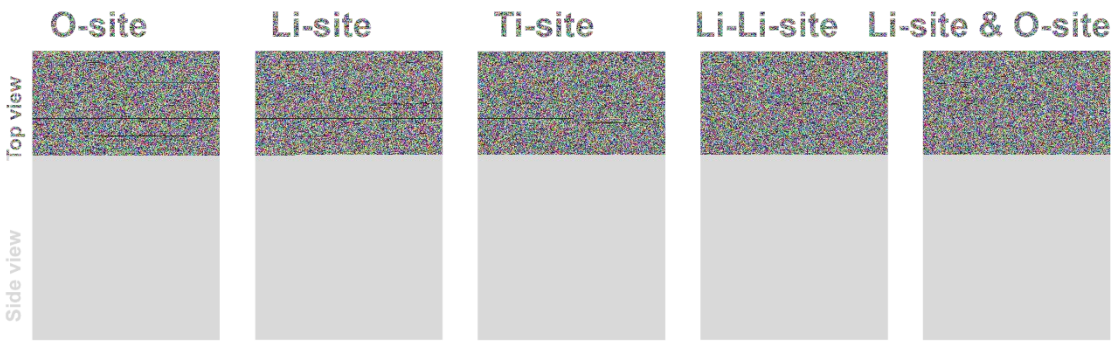

Figure S12. Optimized geometries of Li on $Li_4Ti_5O_{12}$ Li top (111) slab model surfaces and corresponding adsorption energies, respectively. The atoms are colored as follow: Li is green, Ti is blue, C is grey, and O is red.

Figure S13. Optimized geometries of Li on Ti_3C_2 (001) slab model surfaces and corresponding adsorption energies, respectively. The atoms are colored as follow: Li is green, Ti is blue, and C is grey.

Figure S14. Optimized geometries of Li on Cu (111) slab model surfaces and corresponding adsorption energies, respectively. The atoms are colored as follow: Li is green and Cu is navy.

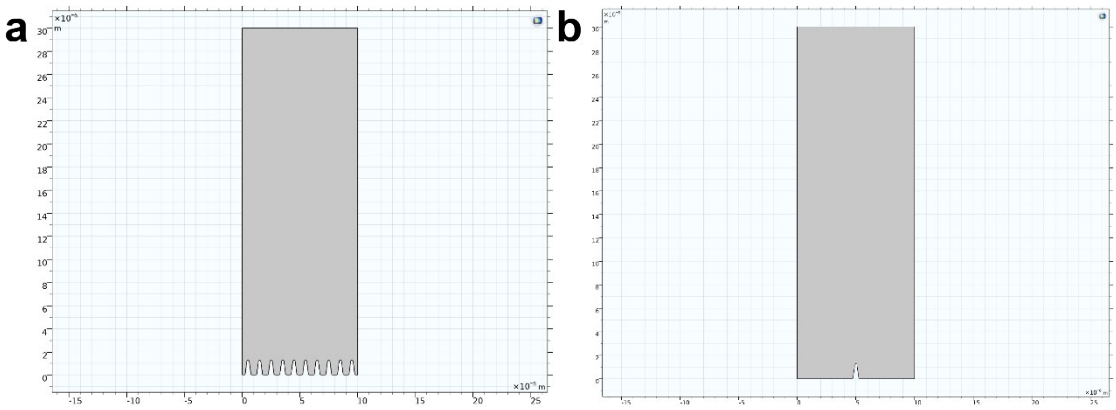

Figure S15. The simulated electrodes geometry in COMSOL for (a) LTO/Ti_3C_2/Cu and (b) bare Cu or Ti_3C_2/Cu electrodes.

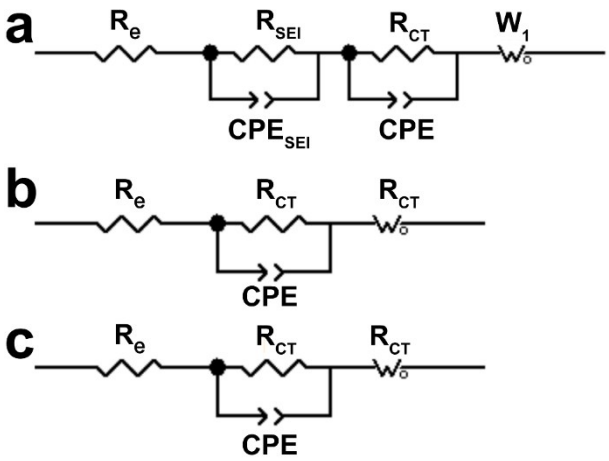

Figure S16. Equivalent circuit fitting for the Nyquist plot of (a) LTO/Ti_3C_2/Cu and (b) bare Cu or Ti_3C_2/Cu electrodes. R_e: the solution and internal resistances of the electrode material. R_{SEI}: solid-electrolyte interface resistance. R_{ct}: charge transfer resistance. CPE: constant phase angle element. W_1: Warburg impedance.

2.SUPPORTING TABLES

Table S1. Computed adsorption energies (eV) of Li on Ti_3C_2 (001) slab, $Li_4Ti_5O_{12}$ (111) slab, and Cu (111) slab.

$Li_4Ti_5O_{12}$ (Ti top)	Li-site	Ti-site	2 Ti-sites		
$E_{Li4Ti5O12}$	-819.73	-819.73	-824.20		
E_{Li}	-0.29	-0.29	-0.29		
ΔE_{ads}	-2.46	-4.17	-6.33		
$Li_4Ti_5O_{12}$ (Li top)	O-site	Li-site	Ti-site	Li-Li-site	2 O-sites
$E_{Li4Ti5O12}$	-887.44	-887.44	-887.44	-889.90	-889.90
E_{Li}	-0.29	-0.29	-0.29	-0.29	-0.29
ΔE_{ads}	-1.50	-2.16	-0.56	-0.56	-1.58
Ti_3C_2	Top-site	Bridge-site	Hollow-site	2 hollow-sites	2 hollow-sites
E_{Ti3C2}	-697.37	-697.37	-697.37	-699.99	-699.99
E_{Li}	-0.29	-0.29	-0.29	-0.29	-0.29
ΔE_{ads}	-2.20	-2.33	-2.33	-2.06	-2.22
Cu	Top-site	Bridge-site	Hollow-site	2 hollow-sites	
E_{Cu}	-212.73	-212.73	-212.73	-215.41	
E_{Li}	-0.29	-0.29	-0.29	-0.29	
ΔE_{ads}	-2.28	-2.37	-2.38	-2.22	

Table S2. Comparison of Li|Li symmetric battery performances on different reported Li host.

Li host	Current density ($mA \cdot cm^{-2}$)	Depositing capacity ($mAh \cdot cm^{-2}$)	Cycle life (h)	*Ref.*
LTO/Ti_3C_2/Cu	1	1	2000	*This work*
Wrinkled graphene cages	1	1	280	S1
Cu@NPCN	1	1	800	S2
PRGOC	1	1	800	S3
rGO	1	1	500	S4
Zn/$Cu_{0.7}Zn_{0.3}$/CF	2.5	1.5	1200	S5
Crumpled Graphene Ball	0.5	1	750	S6
N-doped graphitic carbon foams	2	1	1200	S7

Table S3. Comparison of the full battery performances between this work and other reported works.

Anode	Cathode activity mass loading ($mg \cdot cm^{-2}$)	Current density (C)	Initial capacity ($mAh \cdot g^{-1}$)	Cycle capacity ($mAh \cdot g^{-1}$) (cycles)	*Ref.*
Li/LTO/Ti_3C_2/Cu	5 (LFP)	0.2	154	109(200^{th})	*This work*
Wrinkled graphene cages	9 (LFP)	0.5	120	100(120^{th})	S1
Carbon modified Ni foam	8 (LFP)	0.2	145	93(400^{th})	S8
Li/LTO/Ti_3C_2/Cu	2 (S)	0.5	1076	448(1000^{th})	*This work*
CF/AG-Li	1.7 (S)	0.5	785	505(400^{th})	S9
GZCNT	2.5 (S)	0.2	1200	692(200^{th})	S10
Li_xSi/graphene foil	1 (S)	0.5	1086	858(110^{th})	S11
CFC/Co_3O_4-NC	1.8 (S)	0.5	953	578(200^{th})	S12

REFERENCES

1. H. Wang, Y. Li, Y. Li, Y. Liu, D. Lin, C. Zhu, G. Chen, A. Yang, K. Yan, H. Chen, Y. Zhu, J. Li, J. Xie, J. Xu, Z. Zhang, R. Vila, A. Pei, K. Wang and Y. Cui, *Nano Lett.*, 2019, **19**, 1326-1335.
2. F. Pei, A. Fu, W. Ye, J. Peng, X. Fang, M. S. Wang and N. Zheng, *ACS Nano*, 2019, **13**, 8337-8346.
3. Y. Liu, S. Zhang, X. Qin, F. Kang, G. Chen and B. Li, *Nano Lett.*, 2019, **19**, 4601-4607
4. N. Li. K. Zhang, K. Xie, W. Wei, Y. Gao, M. Bai, Y. Gao, Q. Hou, C. Shen, Z. Xia and B. Wei, *Adv. Mater.*, 2019, **32**, 1907079.
5. Y. Cheng, X. Ke, Y. Chen, X. Huang, Z. Shi and Z. Guo, *Nano Energy*, 2019, **63**.
6. S. Liu, A. Wang, Q. Li, J. Wu, K. Chiou, J. Huang and J. Luo, *Joule*, 2018, **2**, 184-193.
7. L. Liu, Y. X. Yin, J. Y. Li, S. H. Wang, Y. G. Guo and L. J. Wan, *Adv. Mater.*, 2018, **30**.
8. H. Ye, S. Xin, Y. X. Yin, J. Y. Li, Y. G. Guo and L. J. Wan, *J. Am. Chem. Soc.*, 2017, **139**, 5916-5922.
9. R. Zhang, X. Chen, X. Shen, X.-Q. Zhang, X.-R. Chen, X.-B. Cheng, C. Yan, C.-Z. Zhao and Q. Zhang, *Joule*, 2018, **2**, 764-777.
10. H. Zhang, X. Liao, Y. Guan, Y. Xiang, M. Li, W. Zhang, X. Zhu, H. Ming, L. Lu, J. Qiu, Y. Huang, G. Cao, Y. Yang, L. Mai, Y. Zhao and H. Zhang, *Nat. Commun.*, 2018, **9**, 3729.
11. J. Zhao, G. Zhou, K. Yan, J. Xie, Y. Li, L. Liao, Y. Jin, K. Liu, P. C. Hsu, J. Wang, H. M. Cheng and Y. Cui, *Nat. Nanotechnol.*, 2017, **12**, 993-999.
12. G. Jiang, N. Jiang, N. Zheng, X. Chen, J. Mao, G. Ding, Y. Li, F. Sun and Y. Li, *Energy Storage Mater.*, 2019, **23**, 181-189.